



Bandit Algorithm Driven by a Classical Random Walk and a Quantum Walk

Tomoki Yamagami ^{1,*}
André Röhm ¹

Etsuo Segawa ²
Ryoichi Horisaki ¹

Takatomo Mihana ¹
Makoto Naruse ¹

¹ Department of Information Physics and Computing, Graduate School of Information Science and Technology,
The University of Tokyo, 7-3-1 Hongo, Bunkyo, Tokyo 113-8656, Japan.

² Graduate School of Environment and Information Sciences, Yokohama National University,
79-1 Tokiwadai, Hodogaya, Yokohama, Kanagawa 240-8501, Japan.

* Corresponding author. Email: yamagami-tomoki-qwb@g.ecc.u-tokyo.ac.jp

Abstract

Quantum walks (QWs) have the property that classical random walks (RWs) do not possess—coexistence of linear spreading and localization—and this property is utilized to implement various kinds of applications. This paper proposes a quantum-walk-based algorithm for multi-armed-bandit (MAB) problems by associating the two operations that make MAB problems difficult—exploration and exploitation—with these two behaviors of QWs. We show that this new policy based on the QWs realizes high performance compared with the corresponding RW-based one.

Keywords: quantum walk; bandit algorithm; exploration-exploitation trade-off; decision-making

1 Introduction

A quantum walk (QW) is the quantum counterpart of the classical random walk (RW) [1–4], which includes the effects of quantum superposition or time evolution. In classical RWs, a random walker (RWER) selects in which direction to go probabilistically at each time step, and thus one can track where the RWER is at any time step. On the other hand, in QWs, one cannot tell where a quantum walker (QWER) exists during the time evolution, and the location is determined only after conducting the measurement.

QWs have the property that classical RWs do not possess: coexistence of *linear spreading* and *localization* [5, 6]. As a result, QWs show probability distributions that are totally different from those of random walks, which weakly converge to normal distributions. The former behavior, linear spreading, means that the standard deviation of the probability distribution of measurement of quantum walkers (QWers) grows in proportion to the run time t . In the case of discrete-time RWs on a one-dimensional lattice \mathbb{Z} , denoting the random variable of the position where a walker is measured at time $t \in \mathbb{N}_0 = \mathbb{N} \cup \{0\}$ by $X_t^{(\text{RW})}$, then the standard deviation is $\mathbb{D}[X_t^{(\text{RW})}] = O(\sqrt{t})$. On the other hand, in discrete-time QWs on \mathbb{Z} , the standard deviation of a walker’s position at time t is $\mathbb{D}[X_t^{(\text{QW})}] = O(t)$, and thus discrete-time QWs outperform RWs in terms of the propagation velocity [7]. The latter behavior, localization, implies that the probability is distributed at a particular position no matter how long the walk runs. In the classical RWs, the probability distribution gets flat despite keeping a bell-shaped curve; that is, localization is not observed.

QWs were first introduced in the field of quantum information theory [7–9]. The idea of weak convergence, which is frequently used in probability theory, was brought in to show the property of QWs [10, 11], and since then, quantum walks have been actively studied from both fundamental and applied perspectives. In fundamental fields, there have been many attempts to analyze these evolution models mathematically [12–20] due to varying behavior of QWs depending on the conditions or settings of time and space. In applied fields, their unique behavior is useful for implementing quantum structures or quantum analogs of existing models;

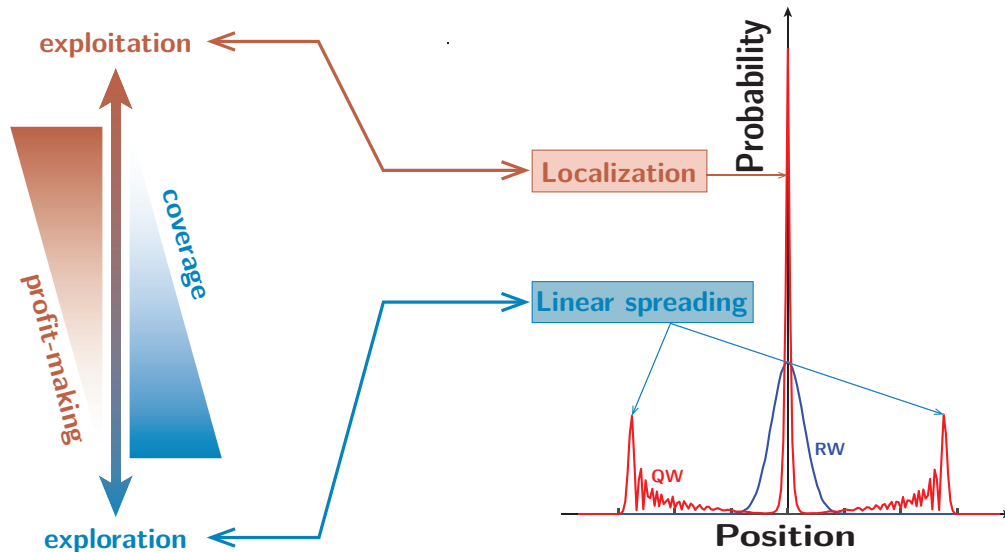


Figure 1: Association between the behaviors of quantum walks (linear spreading and localization) and the operations in MAB problems (exploration and exploitation).

therefore, various QW-based models have been considered for subjects such as time-series analysis [21], topological insulators [22, 23], radioactive waste reduction [24, 25], and optics [26, 27]. In addition, the contribution to quantum information technology is becoming more prominent these days. QWs have been applied not only to the principle of technologies such as quantum search, quantum teleportation [28, 29], and quantum key distribution [30] but also to the implementation of quantum gates themselves [31, 32].

This paper proposes a new solution scheme for multi-armed bandit (MAB) problems [33] using quantum walks. In MAB problems, we consider a situation where there are multiple slot machines in an environment, each gives a reward with a probability allocated to it, and an agent iterates the selection of slot machines and probabilistic gain of the rewards and tries to maximize the total reward. Initially, the agent has no information about the probability of giving rewards, especially which slot machine has the maximum probability, which we call the best slot machine. Thus it is required to accumulate such information through a certain number of selections, an action which we call *exploration*. On the other hand, too much exploration will use up the opportunities for selecting the better slot machines that have already been found; that is, it is also necessary to spend some rounds to bet on slot machines that are reliable based on the information obtained, which we call *exploitation*. The difficulty of MAB problems occurs under the balance between these two operations, known as the *exploration-exploitation trade-off* [34].

In our study, we address this dilemma by utilizing the unique property of QWs, i.e., the coexistence of linear spreading and localization. More precisely, we combine exploration with linear spreading, and exploitation with localization, as shown in Figure 1. By utilizing linear spreading, we intend to cover the whole environment and prevent us from missing some slot machines. In addition, by applying localization, we intend to mark slot machines that should be recommended with a high probability distribution. This paper introduces a QW-based algorithm for MAB problems, which realizes these combinations. Specifically, we conduct three-state site-dependent QWs on a cycle. Giving three states to QWs enables us to obtain a high existence probability on the initial position of a QWer. In addition, site-dependent coin matrices make it possible to trap or dam the QWer on certain vertices. By taking advantage of them, we attempt to make a high probability on a vertex whose slot machine should be recommended. In addition, we construct a random-walk-based algorithm that does not possess linear spreading and localization and compare the performance between these two models. This comparison reveals that linear spreading and localization in the QW-based model enhance the performance in solving MAB problems.

The rest of this paper is organized as follows. In Section 2, we introduce a system of discrete-time quantum walks on a cycle, which is utilized to construct the algorithm for MAB problems. Then, Section 3 proposes a QW-based algorithm for MAB problems. In Section 4, we show some results for numerical simulations

of this QW-based model, where we construct an RW-based model corresponding to the QW-based one and compare the performance between the two models. Section 5 concludes this paper and discusses the future possibilities of our work.

2 Quantum Walk on Cycles

The QW model, which is applied in our study, is a three-state QW on a cycle, which can be naturally reduced to a finite space from the one-dimensional lattice model [5], see for example [17, 35, 36]. Let us explain the definition in detail as follows.

Assume that cycle \mathcal{C}_N is composed of N vertices and edges. Here vertices are labelled by set $V_N := \{0, 1, \dots, N-1\}$, and the label is ordered clockwise. Thus, the set of edges is given by $E_N := \{\{x, x+1\} \mid x \in V_N\}$, where one applies addition and subtraction modulo N to V_N ; i.e., $(N-1)+1 \equiv 0$ and $0-1 \equiv N-1$. In other words, V_N is isometric to $\mathbb{Z}/N\mathbb{Z}$.

The space of our QW is defined in a compound Hilbert space consisting of the position Hilbert space $\mathcal{H}_P = \text{span}\{|x\rangle \mid x \in V_N\}$ and the coin Hilbert space $\mathcal{H}_C = \text{span}\{|-\rangle, |O\rangle, |+\rangle\}$ with $|-\rangle = [1 \ 0 \ 0]^T$, $|O\rangle = [0 \ 1 \ 0]^T$, and $|+\rangle = [0 \ 0 \ 1]^T$, where superscript T on a matrix represents the transpose of it. Here $|x\rangle$ for $x \in V_N$ is the unit vector corresponding to position x , and the relation $\langle y|x\rangle = \delta_y(x)$ holds for any $x, y \in V_N$, where $\delta_y(x)$ is the delta function:

$$\delta_y(x) = \begin{cases} 1 & (x = y) \\ 0 & (\text{otherwise}) \end{cases} . \quad (2.1)$$

In addition, vectors $|-\rangle$, $|O\rangle$, and $|+\rangle$ correspond to the inner states of QWers. Note that $\mathcal{H}_P \simeq \mathbb{C}^N$ and $\mathcal{H}_C \simeq \mathbb{C}^3$. Then, the whole system is described by

$$\mathcal{H}_{PC} = \mathcal{H}_P \otimes \mathcal{H}_C = \text{span}\{|x\rangle \otimes |J\rangle \mid x \in V_N, J \in \{\pm, O\}\}. \quad (2.2)$$

Then the total state of our QW at time $t \in \mathbb{N}_0$ is represented as follows: there exists $|\psi^{(t)}(x)\rangle \in \mathbb{C}^3$ for each $x \in V_N$ such that

$$|\Psi^{(t)}\rangle = \sum_{x \in V_N} |x\rangle \otimes |\psi^{(t)}(x)\rangle \in \mathcal{H}_{PC}. \quad (2.3)$$

Here, $t \in \mathbb{N}_0$ represents time step of QWs, and $|\psi^{(t)}(x)\rangle \in \mathbb{C}^3$ is called the probability amplitude vector at position $x \in V_N$ at run time t . We set the initial state as

$$|\Psi^{(0)}\rangle = |\Phi\rangle := |s\rangle \otimes |\varphi\rangle, \quad (2.4)$$

where $s \in V_N$, and $|\varphi\rangle \in \mathbb{C}^3$ is a constant vector with $\|\varphi\| = 1$.

Now, we introduce the time evolution of $|\Psi^{(t)}\rangle$ by

$$|\Psi^{(t+1)}\rangle = U |\Psi^{(t)}\rangle. \quad (2.5)$$

Here U is the unitary operator, referred to as the time evolution operator, and is composed of shift operator S and coin operator C :

$$U = SC, \quad (2.6)$$

and S and C are given by

$$S = S^\dagger \otimes |-\rangle\langle -| + I_N \otimes |O\rangle\langle O| + S \otimes |+\rangle\langle +| \quad (2.7)$$

and

$$C = \sum_{x \in V_N} (|x\rangle\langle x| \otimes C(x)). \quad (2.8)$$

Here S is defined as

$$S = \sum_{x \in V_N} |x+1\rangle\langle x| \quad (2.9)$$

and represents the clockwise transition, and then

$$S^\dagger = \sum_{x \in V_N} |x-1\rangle\langle x| \quad (2.10)$$

indicates the anti-clockwise transition. The identity matrix I_N corresponds to staying on the same position. Here, note that $N \equiv 0$ on $V_N (\simeq \mathbb{Z}/N\mathbb{Z})$; that is, for example, in the case of $N = 4$,

$$S = |1\rangle\langle 0| + |2\rangle\langle 1| + |3\rangle\langle 2| + |0\rangle\langle 3| \quad (2.11)$$

and

$$S^\dagger = |3\rangle\langle 0| + |0\rangle\langle 1| + |1\rangle\langle 2| + |2\rangle\langle 3|. \quad (2.12)$$

$C(x)$ is a unitary matrix called a *coin matrix*, which is defined as follows:

$$C(x) = \begin{bmatrix} -\frac{1 + \cos \theta(x)}{2} & \frac{\sin \theta(x)}{\sqrt{2}} & \frac{1 - \cos \theta(x)}{2} \\ \frac{\sin \theta(x)}{\sqrt{2}} & \cos \theta(x) & \frac{\sin \theta(x)}{\sqrt{2}} \\ \frac{1 - \cos \theta(x)}{2} & \frac{\sin \theta(x)}{\sqrt{2}} & -\frac{1 + \cos \theta(x)}{2} \end{bmatrix} \quad (2.13)$$

with $\theta(x) \in [0, 2\pi)$ for all $x \in V_N$. Note that, in the case of $\cos \theta(x) = -1/3$, $C(x)$ is reduced to the Grover matrix, which is important in quantum search.

Let us explain the equivalent expression for the time evolution operator U , which is useful to understand the dynamics of our QW, as follows: by applying the property of the Kronecker product, we have

$$U = \sum_{x \in V_N} (|x-1\rangle\langle x| \otimes P(x) + |x\rangle\langle x| \otimes R(x) + |x+1\rangle\langle x| \otimes Q(x)), \quad (2.14)$$

where

$$P(x) = |- \rangle\langle - | C(x) = \begin{bmatrix} -\frac{1 + \cos \theta(x)}{2} & \frac{\sin \theta(x)}{\sqrt{2}} & \frac{1 - \cos \theta(x)}{2} \\ 0 & 0 & 0 \\ 0 & 0 & 0 \end{bmatrix}, \quad (2.15)$$

$$Q(x) = |+\rangle\langle +| C(x) = \begin{bmatrix} 0 & 0 & 0 \\ 0 & 0 & 0 \\ \frac{1 - \cos \theta(x)}{2} & \frac{\sin \theta(x)}{\sqrt{2}} & -\frac{1 + \cos \theta(x)}{2} \end{bmatrix}, \quad (2.16)$$

$$R(x) = |0\rangle\langle 0| C(x) = \begin{bmatrix} 0 & 0 & 0 \\ \frac{\sin \theta(x)}{\sqrt{2}} & \cos \theta(x) & \frac{\sin \theta(x)}{\sqrt{2}} \\ 0 & 0 & 0 \end{bmatrix}. \quad (2.17)$$

The matrices $P(x)$, $Q(x)$, and $R(x)$ are considered to be the decomposition elements of $C(x)$; that is, the relation $P(x) + Q(x) + R(x) = C(x)$ holds. They correspond to the matrix-valued weight of a transition in clockwise, a transition in anti-clockwise, and remaining in place respectively, as shown in Figure 2.

By Eqs. (2.5) and (2.14), we have

$$|\psi^{(t+1)}(x)\rangle = P(x+1) |\psi^{(t)}(x+1)\rangle + R(x) |\psi^{(t)}(x)\rangle + Q(x-1) |\psi^{(t)}(x-1)\rangle. \quad (2.18)$$

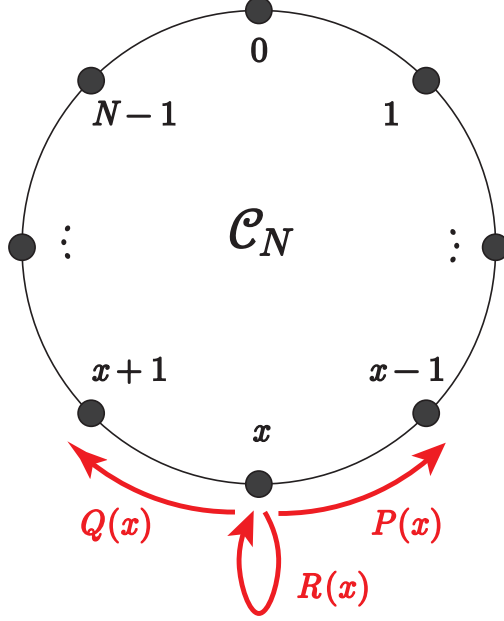


Figure 2: Quantum walks on cycle \mathcal{C}_N and matrices $P(x)$, $Q(x)$, and $R(x)$ for time evolution.

Moreover, from the initial state (2.4), there exists a 2-dimensional matrix $\Xi^{(t)}(x)$ such that

$$|\psi^{(t)}(x)\rangle = \Xi^{(t)}(x) |\varphi\rangle. \quad (2.19)$$

Here $\Xi^{(t)}(x)$ describes the weight of all the possible paths from the origin to the position x at run time t . From Eq. (2.18), the following relation holds:

$$\Xi^{(t+1)}(x) = P(x+1)\Xi^{(t)}(x+1) + R(x)\Xi^{(t)}(x) + Q(x-1)\Xi^{(t)}(x-1). \quad (2.20)$$

Finally, the measurement probability of the particle at position x at run time t , denoted by $\mu^{(t)}(x)$, is given by

$$\mu^{(t)}(x) := \|\psi^{(t)}(x)\|^2. \quad (2.21)$$

Setting random variable X_t following the distribution $\mu^{(t)}$, we call X_t the position of a QWer at time t . This definition is based on the Born probability interpretation in quantum mechanics. Note that for any $t \in \mathbb{N}_0$, the following is satisfied:

$$\sum_{x \in V_N} \mu^{(t)}(x) = \sum_{x \in V_N} \|\psi^{(t)}(x)\|^2 = 1. \quad (2.22)$$

3 Quantum-Walk-Based Model for MAB Problems

We consider N -armed bandit problem with cycle \mathcal{C}_N ; each vertex $x \in V_N$ is given a slot machine which gives a reward with the probability $p(x)$. In the following, we identify the number of vertices and those of the slot machines; for example, we call the slot machine on the vertex x slot machine x . In addition, we call probability $p(x)$ the *success probability of slot machine x* . Moreover, we denote the slot machine with the best success probability in V_N by x^* ; that is,

$$x^* = \arg \max_{x \in V_N} p(x), \quad (3.1)$$

and we call it the *best slot machine*.

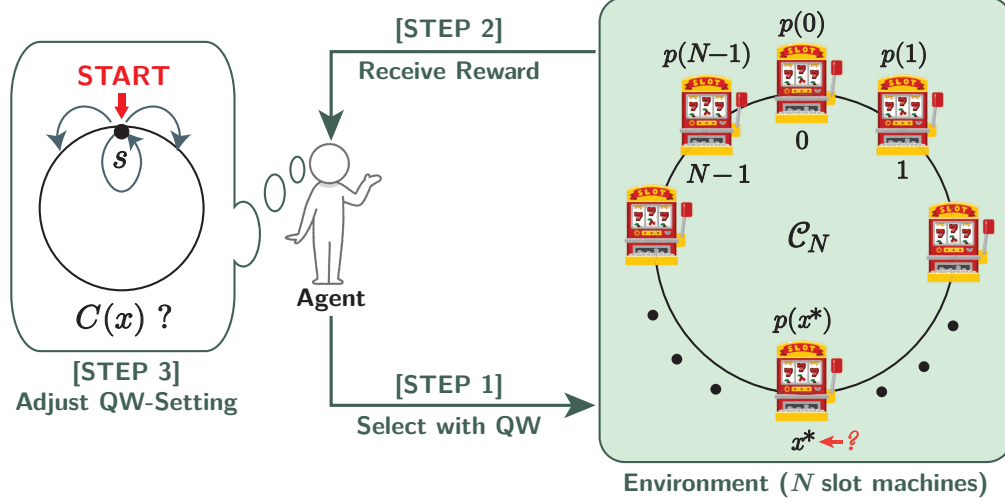


Figure 3: Single decision on the quantum-walk-based model for MAB problems

The principle consists of the following four steps: **[STEP 0]** initializing the quantum-walk-setting, **[STEP 1]** running random walks, **[STEP 2]** playing the selected slot machine, and **[STEP 3]** updating the setting of quantum walks. After finishing **[STEP 3]**, the process returns to **[STEP 1]**. We call a series of the last three steps (**[STEP 1–3]**, shown in Figure 3) a *decision*, and decisions are iterated J times over a run. Here, we use the following notations:

- $|\Phi_j\rangle \in \mathcal{H}_{\text{PC}}$: Initial state of quantum walk on the j -th decision.
- $s_j \in V_N$: Initial position of quantum walk on the j -th decision. The relation $|\Phi_j\rangle = |s_j\rangle \otimes |\varphi\rangle$ holds.
- $\theta_j(x) \in [0, 2\pi)$: Parameter of Eq. (2.13) on vertex x on the j -th decision; then the coin matrix there is $C(x)$.
- $\hat{x}_j \in V_N$: Vertex (slot machine) measured on the j -th decision.
- $\hat{r}_j \in \{0, 1\}$: Reward on the j -th decision, which follows the Bernoulli distribution $\text{Ber}(p(\hat{x}_j))$:

$$\hat{r}_j := \begin{cases} 1 & (\text{with prob. } p(\hat{x}_j)) \\ 0 & (\text{with prob. } 1 - p(\hat{x}_j)) \end{cases} . \quad (3.2)$$

- $H_j(x)$: Number of decisions that slot machine x is selected until the j -th decision.
- $L_j(x)$: Number of decisions that slot machine x gives the reward until the j -th decision.
- $\hat{p}_j(x)$: Empirical probability that slot machine x gives the reward on the j -th decision:

$$\hat{p}_j(x) = \begin{cases} \frac{L_j(x)}{H_j(x)} & (H_j(x) \neq 0) \\ 0 & (H_j(x) = 0) \end{cases} . \quad (3.3)$$

[STEP 0] QW-setting initialization

For the first decision, the settings of the quantum walk are determined as follows:

- Initial state $|\Phi_1\rangle$: First register $|s_1\rangle$ is probabilistically determined by the uniform distribution on V_N .
- Parameter of coin matrices: $\theta_1(x) = \theta^\circ \in [0, 2\pi)$ for all $x \in V_N$.

After finishing this step, the run iterates the following three steps.

[STEP 1] Quantum walk

Quantum walks are run over T time steps with the initial position s_j and the parameter $\theta_j(x)$. After running T steps of time evolution, the QWer is measured to obtain the value $\hat{x}_j \in V_N$ following probability distribution $\mu^{(T)}(x)$.

[STEP 2] Slot machine play

The slot machine $\hat{x}_j \in V_N$ obtained at **[STEP 1]** is played. Then, the reward ($\hat{r}_j = 1$) is obtained with probability $p(\hat{x}_j)$.

Here $H_j(x)$ s and $L_j(x)$ s are updated. First, the H -value on \hat{x}_j is incremented:

$$H_j(\hat{x}_j) = H_{j-1}(\hat{x}_j) + 1. \quad (3.4)$$

If $\hat{r}_j = 1$, the L -value on \hat{x}_j is also incremented (otherwise, the value is maintained):

$$L_j(\hat{x}_j) = \begin{cases} L_{j-1}(\hat{x}_j) + 1 & \text{(with prob. } p(\hat{x}_j)) \\ L_{j-1}(\hat{x}_j) & \text{(with prob. } 1 - p(\hat{x}_j)) \end{cases}. \quad (3.5)$$

For $x \neq \hat{x}_j$, the H - and L -values are maintained:

$$H_j(x) = H_{j-1}(x), \quad (3.6)$$

$$L_j(x) = L_{j-1}(x). \quad (3.7)$$

Based on that, $\hat{p}_j(x)$ s are updated.

[STEP 3] QW-setting adjustment

Using the new $\hat{p}_j(x)$ s, the settings of quantum walks for the next decision are updated. The new initial state is defined as

$$|\Phi_{j+1}\rangle = |s_j\rangle \otimes |\varphi\rangle, \quad (3.8)$$

where s_j is the provisionally best machine:

$$s_j = \arg \max_{x \in V_N} \hat{p}_j(x). \quad (3.9)$$

Moreover, the new parameters of the coin matrices are determined as

$$\theta_{j+1}(x) = \theta^\circ \exp(-a \cdot \hat{p}_j(x)^b) \quad (3.10)$$

where $a, b > 0$, and θ° is defined in **[STEP 0]**. After this step, the process returns to **[STEP 1]**.

4 Numerical Simulations

In this section, we give some simulation results for our proposed model. Assume that runs are conducted in parallel K times, and each run is labelled by the set $\{1, 2, \dots, K\}$. We indicate that the parameters are in the k -th run by subscript next to the number of iterations; for example, the reward on the j -th decision in the k -th run is denoted by $\hat{r}_{j,k}$.

To estimate the efficiency of our proposed model, we need to investigate how the results change if one confiscates linear spreading and localization from the model. Thus, we construct the random-walk-based model for MAB problems corresponding to the QW-based model and compare the performance between QW- and RW-based models.

As figures-of-merit, we define quantities $M(j)$, $\rho(j)$, and $\text{CDR}(j)$:

$$M(j) := \frac{1}{K} \sum_{k=1}^K \sum_{\ell=1}^j \hat{r}_{\ell, k}, \quad (4.1)$$

$$\rho(j) := \frac{1}{K} \sum_{k=1}^K \sum_{\ell=1}^j (p(x^*) - p(\hat{x}_{\ell, k})), \quad (4.2)$$

$$\text{CDR}(j) := \frac{1}{K} \sum_{k=1}^K \delta_{x^*}(\hat{x}_{j, k}). \quad (4.3)$$

$M(j)$ indicates the mean of *total rewards* until the j -th decision over K runs. The aim of the proposed model is to make $M(j)$ as large as possible. $\rho(j)$ is the mean of *cumulative regret* until the j -th decision over K runs. The cumulative regret is equal to the difference in expectations of total reward between the case where only the best machine is selected until the j -th decision and that of actual selections until then. $\text{CDR}(j)$ is the *correct decision rate* of the j -th decision, which is the ratio of the number of runs in selecting the best slot machine to the total number of runs K . Herein δ_y for $y \in V_N$ is the delta function defined by Eq. (2.1).

4.1 Random-Walk-Based Model

Here we introduce discrete-time random walks on cycle \mathcal{C}_N introduced in Section 2. We assume that the position of a walker is determined as follows:

- A walker initially exists on position $s \in V_N$.
- At each time step, a walker on position x moves one unit clockwise with probability $q(x)$, moves one unit anti-clockwise with probability $q(x)$ or stays on the current position with probability $1 - 2q(x)$.

Note that the probabilities of moving clockwise and anti-clockwise are equal to each other in this paper, and $q(x)$ should satisfy $0 \leq q(x) \leq 1/2$ under this condition. In the case of $q(x) = 1/2$ for all $x \in V_N$, this setting is equivalent to the simple random walk on cycles.

For $\mathbb{N}_0 = \{0, 1, \dots\}$, let $\{X_t\}_{t \in \mathbb{N}_0}$ be the sequence of random variables that represent the position of a walker right after time step t , and we denote the probability that a walker is on position x right after time step t by $\nu^{(t)}(x)$:

$$\nu^{(t)}(x) = \mathbb{P}(X_t = x). \quad (4.4)$$

Then, based on the rules of a walker above, $\nu^{(t)}(x)$ is determined by the following equations:

$$\nu^{(0)}(x) = \delta_s(x) = \begin{cases} 1 & (x = s) \\ 0 & (\text{otherwise}) \end{cases}, \quad (4.5)$$

$$\nu^{(t+1)}(x) = q(x+1)\nu^{(t)}(x+1) + (1 - 2q(x))\nu^{(t)}(x) + q(x-1)\nu^{(t)}(x-1). \quad (4.6)$$

We recall that $V_N \simeq \mathbb{Z}/N\mathbb{Z}$.

We consider an N -armed bandit problem with cycle \mathcal{C}_N labeled by $V_N \simeq \mathbb{Z}/N\mathbb{Z}$ equally to the QW-based model. The principle consists of the following four steps: **[STEP 0]** initializing the random-walk-setting, **[STEP 1]** running random walks, **[STEP 2]** playing the selected slot machine, and **[STEP 3]** updating the setting of random walks. After finishing **[STEP 3]**, the process returns to **[STEP 1]**. We call the series of the last three steps (**[STEP 1–3]**) a *decision*, and decisions are iterated J times over a run. Here, we use the following notations:

- $s_j \in V_N$: Initial position of random walk on the j -th decision.
- $q_j(x) \in [0, 1/2]$: Clockwise-transition probability and anti-clockwise-transition probability on the j -th decision.
- $\hat{x}_j \in V_N$: Vertex (slot machine) measured on the j -th decision.

- $\hat{r}_j \in \{0, 1\}$: Reward on the j -th decision. This value is probabilistically determined by the Bernoulli distribution $\text{Ber}(p(\hat{x}_j))$; that is,

$$\hat{r}_j := \begin{cases} 1 & (\text{with prob. } p(\hat{x}_j)) \\ 0 & (\text{with prob. } 1 - p(\hat{x}_j)) \end{cases} . \quad (4.7)$$

- $H_j(x)$: Number of decisions where the slot machine x is selected until the j -th decision.
- $L_j(x)$: Number of decisions where the slot machine x gives the reward until the j -th decision.
- $\hat{p}_j(x)$: Empirical probability that the slot machine x gives the reward on the j -th decision:

$$\hat{p}_j(x) = \begin{cases} \frac{L_j(x)}{H_j(x)} & (H_j(x) \neq 0) \\ 0 & (H_j(x) = 0) \end{cases} . \quad (4.8)$$

[STEP 0] RW-setting initialization

For the first decision, the settings of the random walk are determined as follows:

- Initial position s_1 : Probabilistically determined by the uniform distribution on V_N .
- Transition probability: $q_1(x) = q^\circ \in [0, 1/2]$ for all $x \in V_N$.

After finishing this step, the process iterates the following three steps.

[STEP 1] Random walk

Random walks are run over T time steps with the initial position s_j and transition probability $q_j(x)$, and the value $\hat{x}_j \in V_N$ is obtained following probability distribution $\nu^{(T)}(x)$.

[STEP 2] Slot machine play

The slot machine $\hat{x}_j \in V_N$ obtained at [STEP 1] is played. Then, the reward ($\hat{r}_j = 1$) is obtained with probability $p(\hat{x}_j)$.

Here $H_j(x)$ s and $L_j(x)$ s are updated. First, the H -value on \hat{x}_j is incremented:

$$H_j(\hat{x}_j) = H_{j-1}(\hat{x}_j) + 1. \quad (4.9)$$

If $\hat{r}_j = 1$, the L -value on \hat{x}_j is also incremented (otherwise, the value is maintained):

$$L_j(\hat{x}_j) = \begin{cases} L_{j-1}(\hat{x}_j) + 1 & (\text{with prob. } p(\hat{x}_j)) \\ L_{j-1}(\hat{x}_j) & (\text{with prob. } 1 - p(\hat{x}_j)) \end{cases} . \quad (4.10)$$

For $x \neq \hat{x}_j$, the H - and L -values are maintained:

$$H_j(x) = H_{j-1}(x), \quad (4.11)$$

$$L_j(x) = L_{j-1}(x). \quad (4.12)$$

Based on that, $\hat{p}_j(x)$ s are updated.

[STEP 3] RW-setting adjustment

Using the new $\hat{p}_j(x)$ s, the settings of quantum walks are updated for the next decision. The new initial position is defined as

$$s_{j+1} = \arg \max_{x \in V_N} \hat{p}_j(x). \quad (4.13)$$

Moreover, the new transition probabilities are determined as

$$q_{j+1}(x) = q^\circ \exp(-a \cdot \hat{p}_j(x)^b) \quad (4.14)$$

where $a, b > 0$, and q° is defined in [STEP 0]. After this step, the process returns to [STEP 1].

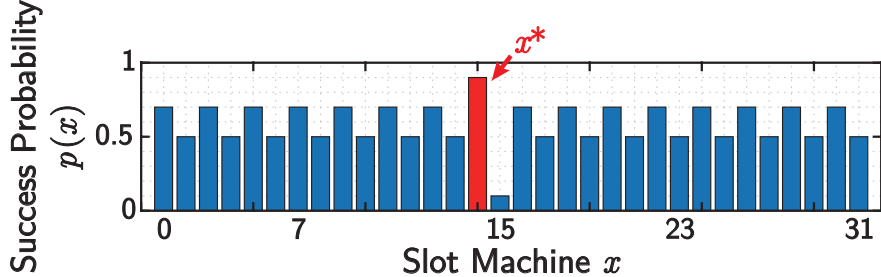


Figure 4: Success probability $p(x)$ for slot machine $x \in V_N$. The number of slot machines N is set to 32, and the best slot machine is $x^* = 14$.

4.2 Comparison of QW-Based Model with RW-Based Model

We compare the performances between the QW- and RW-based algorithms. The parameter values used for this series of simulations are summarized in Table 1. The success probabilities of slot machines are given as shown in Figure 4; that is,

$$p(x) = \begin{cases} 0.9 & (x = 14) \\ 0.1 & (x = 15) \\ 0.7 & (x : \text{even except for } 14) \\ 0.5 & (x : \text{odd except for } 15) \end{cases} \quad (4.15)$$

Herein, the best slot machine is set to $x^* = 14$. Recall that the agent cannot directly access all information regarding the success probabilities of slot machines above. The tuples for the QW- and RW-based models are selected as one of the best performers on each model. The details about parameter-dependencies of both models are found in Appendix A.

The orange and blue curves in Figures 5(a)–(c) demonstrate the performances of QW- and RW-based models as the variations of the mean of total reward $M(j)$, the maximum value of CDR, and the cumulative regret $\rho(j)$ over the number T of time steps of walks for single decision-making, respectively. The total reward and the cumulative regret are taken for the final decision $J = 5000$. The maximum value of CDR is taken over J decisions; that is,

$$\max(\text{CDR}) := \max_{j=1, \dots, J} \text{CDR}(j). \quad (4.16)$$

For $T \geq 4$, we observe that $M(5000)$ and $\max(\text{CDR})$ of the QW-based model outperform those of the RW-based model. On the other hand, for the cumulative regret $\rho(5000)$, the value for the QW-based model is lower than that for the RW-based model. Both results indicate that the performance of the QW-based model is superior to that of the RW-based model. From these figures, we can also confirm the contribution of linear spreading and localization to enhancing performance. First, linear spreading makes the growth of the performance faster; the gradient of the orange curve (QW) at smaller T in $M(5000)$ is larger than that of the blue curve (RW). Second, localization realizes a higher performance limit; $\max(\text{CDR})$ of the QW-based model converges to 1 while that of the RW-based model converges to around 0.95.

Table 1: Parameter values used for numerical simulation of decision making.

Parameter	Symbol	Value
Number of slot machines	N	32
Number of runs	K	500
Number of decisions for a single run	J	5000
Parameters for the QW-based model	(a, b, θ°)	(5, 6, $5\pi/16$)
Parameters for the RW-based model	(a, b, q°)	(9, 6, 0.5)

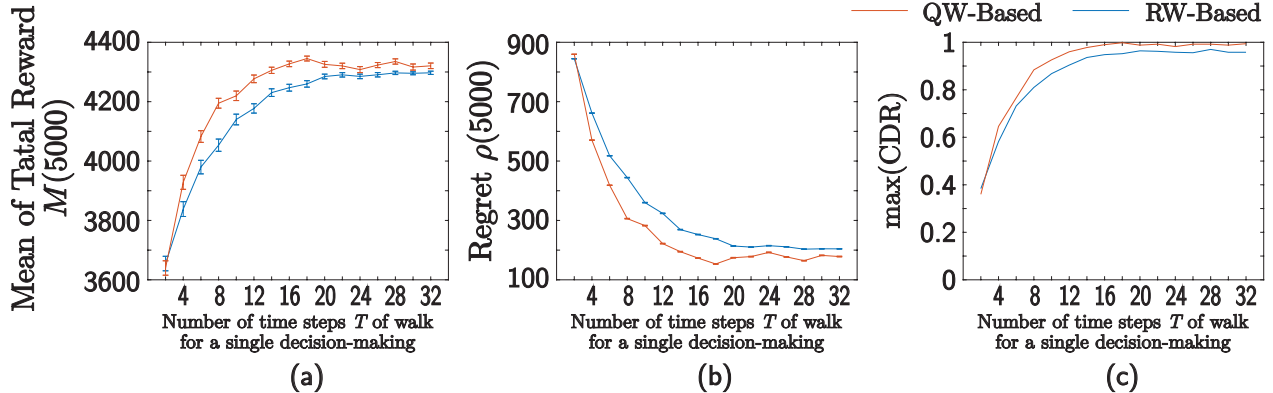


Figure 5: Comparison of (a) mean of total reward $M(J)$, (b) cumulative regret $\rho(J)$, and (c) the maximum value of CDR over the variation of final time step T of walks between QW- and RW-based models. Parameters are determined as shown in Table 1.

5 Conclusion and Discussion

This paper has proposed a new solution scheme for multi-armed bandit (MAB) problems [33] using quantum walks. We addressed the exploration–exploitation dilemma by utilizing the unique property of QWs, i.e., coexistence of linear spreading and localization. More precisely, we combined exploration with linear spreading, and exploitation with localization. By utilizing linear spreading, we intend to cover the whole environment to prevent us from missing some slot machines. In addition, by applying localization, we intend to identify the slot machine that should be recommended with a high probability distribution. We confirmed that the QW-based algorithm introduced in this paper realizes these combinations by comparing it with the corresponding random-walk-based algorithm, which does not possess linear spreading or localization. Here, linear spreading contributes to the growth of the performance over the variation of time steps of the walk for single decision-making, and localization contributes to realizing the higher performance limitation.

The positive results obtained in this study open the possibility for further extensions. First, can we apply this algorithm to the case of multi-agent systems such as competitive or adversarial bandit problems [37–39] with some revision? We will examine its application to the use of coin matrices implemented by multiple registers or to drive walkers on a torus. Also, there are possibilities for constructing application models in the single-agent case. For example, we may construct an evolved version of our model, including a quantum version of the optimal stopping problem. Moreover, the analysis of our model is also important. The difficulty of this work is the dependency of the coin matrices on the position. This matter has been examined [14, 20], but the generalized case is still open. To properly analyze this model, we need to accumulate analytical results for site-dependent quantum walks in the long term.

Appendix A: Parameter-Dependencies of QW- and RW-Based Models

We show (a, b, θ°) -dependency of the QW-based model and (a, b, q°) -dependency of the RW-based model. Here we fix the number T of time steps of the walk for single decision-making to 32. The numbers of slot machines, runs, and decisions for a single run are equal to those of the simulation in Section 4.2; that is, $(N, K, J) = (32, 500, 5000)$.

Figure 6 demonstrates the performance of the QW-based model depending on tuple (a, b, θ°) , which determines phase $\theta(x)$ of coin matrix $C(x)$ defined by Eq. (3.10). We observe that when setting $a = 1$, θ° makes performance worse with violating oscillations. For other cases of a , performance has the tendency to improve over the growth of θ° . Especially, in the case of $b = 6$, $\max(\text{CDR})$ is almost 1 for the sufficiently large θ° as shown in Figure 6(c3), and particularly the case of $(a, b) = (5, 6)$ realizes the better performance. In Section 4.2, we selected tuple $(a, b, \theta^\circ) = (5, 6, 5\pi/16)$ as the representative of this case.

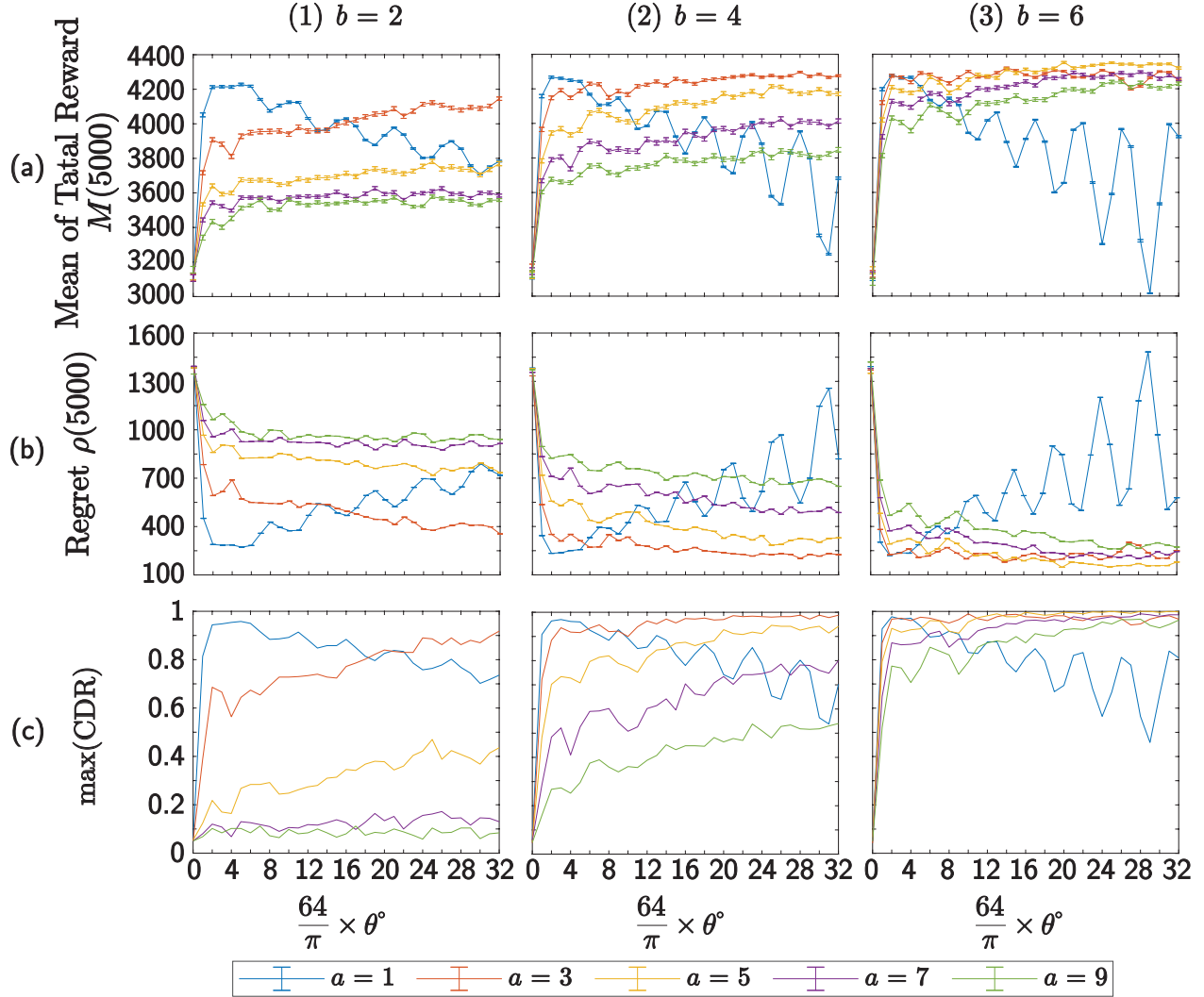


Figure 6: Comparison of the (a) mean of total reward $M(j)$, (b) cumulative regret $\rho(j)$, and (c) the maximum value of CDR.

Figure 7 demonstrates the performance of the RW-based model depending on tuple (a, b, q°) , which determines transition probability $q(x)$ defined by Eq. (4.14). We observe that higher b enables better performance, which makes $q(x)$ sensible to the variation of $\hat{p}(x)$. Besides, the higher b becomes, the higher a is needed to realize better performance. In our results, the best performance is obtained for the case of $(a, b) = (9, 6)$, where $\max(\text{CDR})$ is over 0.95 for $q^\circ \geq 0.25$ in Figure 7(c3). In Section 4.2, we selected tuple $(a, b, q^\circ) = (9, 6, 0.5)$ as the representative of this range.

Acknowledgments: This work was supported by the SPRING program (JPMJSP2108), the CREST project (JPMJCR17N2) funded by the Japan Science and Technology Agency, and Grants-in-Aid for Scientific Research (JP20H00233) and Transformative Research Areas (A) (22H05197) funded by the Japan Society for the Promotion of Science.

Data availability statement: The data that support the findings of this study are available from the corresponding author upon reasonable request.

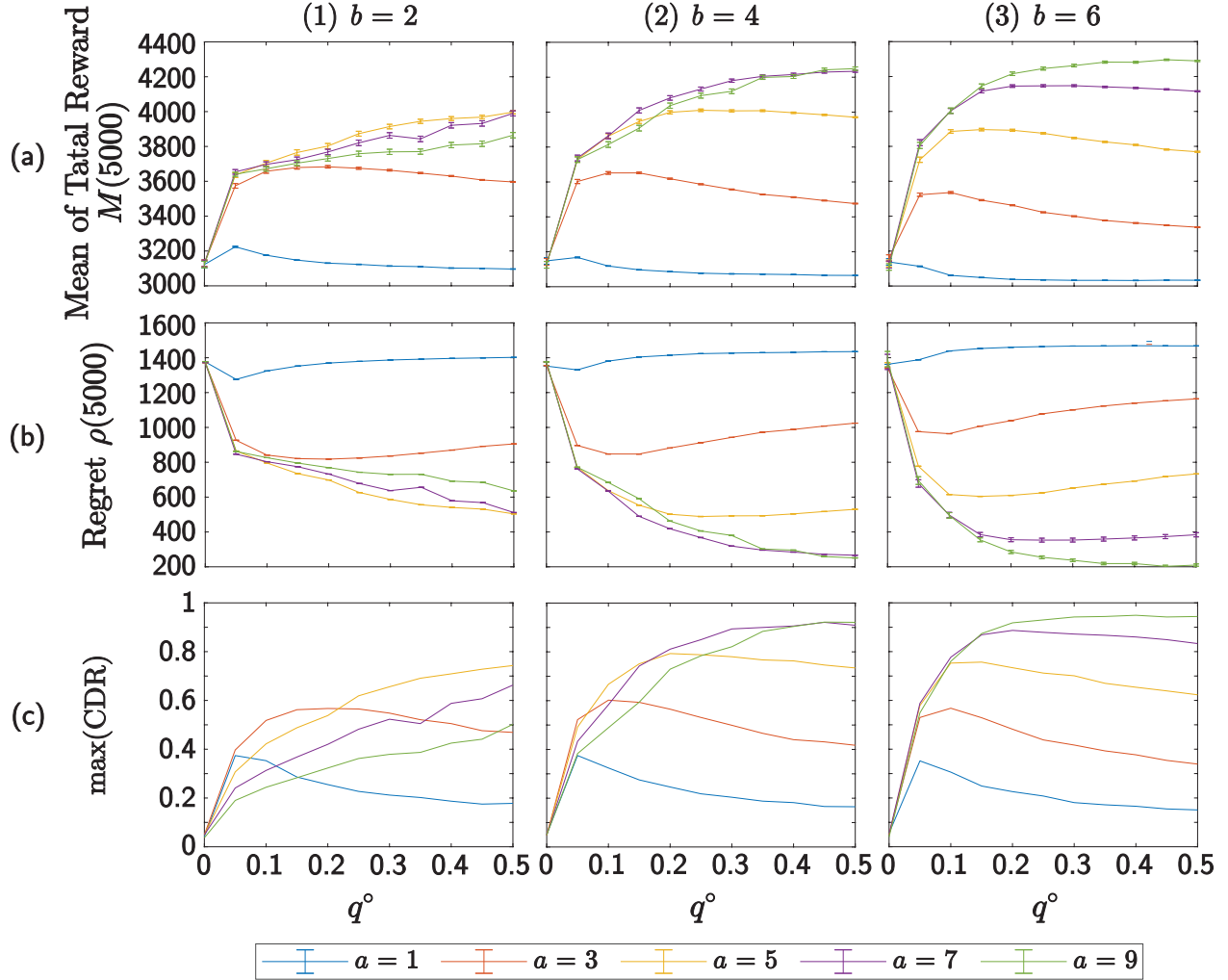


Figure 7: Comparison of the (a) mean of total reward $M(j)$, (b) cumulative regret $\rho(j)$, and (c) the maximum value of CDR.

References

- [1] N. Konno, “Quantum walks,” in *Quantum potential theory*, pp. 309–452, Springer, 2008.
- [2] J. Kempe, “Quantum random walks: an introductory overview,” *Contemporary Physics*, vol. 44, no. 4, pp. 307–327, 2003.
- [3] S. E. Venegas-Andraca, “Quantum walks: a comprehensive review,” *Quantum Information Processing*, vol. 11, no. 5, pp. 1015–1106, 2012.
- [4] V. Kendon, “Decoherence in quantum walks—a review,” *Mathematical Structures in Computer Science*, vol. 17, no. 6, pp. 1169–1220, 2007.
- [5] N. Inui, N. Konno, and E. Segawa, “One-dimensional three-state quantum walk,” *Physical Review E*, vol. 72, no. 5, p. 056112, 2005.
- [6] N. Konno, T. Luczak, and E. Segawa, “Limit measures of inhomogeneous discrete-time quantum walks in one dimension,” *Quantum information processing*, vol. 12, no. 1, pp. 33–53, 2013.

- [7] A. Ambainis, E. Bach, A. Nayak, A. Vishwanath, and J. Watrous, “One-dimensional quantum walks,” in *Proceedings of the thirty-third annual ACM symposium on Theory of computing*, pp. 37–49, 2001.
- [8] S. P. Gudder, *Quantum Probability*. Elsevier Science, 1988.
- [9] Y. Aharonov, L. Davidovich, and N. Zagury, “Quantum random walks,” *Phys. Rev. A*, vol. 48, pp. 1687–1690, Aug 1993.
- [10] N. Konno, “Quantum random walks in one dimension,” *Quantum Information Processing*, vol. 1, no. 5, pp. 345–354, 2002.
- [11] N. Konno, “A new type of limit theorems for the one-dimensional quantum random walk,” *Journal of the Mathematical Society of Japan*, vol. 57, no. 4, pp. 1179–1195, 2005.
- [12] N. Konno, “Localization of an inhomogeneous discrete-time quantum walk on the line,” *Quantum Information Processing*, vol. 9, no. 3, pp. 405–418, 2010.
- [13] T. Sunada and T. Tate, “Asymptotic behavior of quantum walks on the line,” *Journal of Functional Analysis*, vol. 262, no. 6, pp. 2608–2645, 2012.
- [14] N. Konno, T. Łuczak, and E. Segawa, “Limit measures of inhomogeneous discrete-time quantum walks in one dimension,” *Quantum information processing*, vol. 12, no. 1, pp. 33–53, 2013.
- [15] J. Bourgain, F. Grünbaum, L. Velázquez, and J. Wilkening, “Quantum recurrence of a subspace and operator-valued schur functions,” *Communications in Mathematical Physics*, vol. 329, no. 3, pp. 1031–1067, 2014.
- [16] A. Suzuki, “Asymptotic velocity of a position-dependent quantum walk,” *Quantum Information Processing*, vol. 15, pp. 103–119, 2016.
- [17] P. Sadowski, J. A. Miszczyk, and M. Ostaszewski, “Lively quantum walks on cycles,” *Journal of Physics A: Mathematical and Theoretical*, vol. 49, no. 37, p. 375302, 2016.
- [18] C. Godsil and H. Zhan, “Discrete-time quantum walks and graph structures,” *Journal of Combinatorial Theory, Series A*, vol. 167, pp. 181–212, 2019.
- [19] C. Cedzich, J. Fillman, T. Geib, and A. Werner, “Singular continuous cantor spectrum for magnetic quantum walks,” *Letters in Mathematical Physics*, vol. 110, no. 6, pp. 1141–1158, 2020.
- [20] C. Kiumi, “Localization of space-inhomogeneous three-state quantum walks,” *Journal of Physics A: Mathematical and Theoretical*, vol. 55, no. 22, p. 225205, 2022.
- [21] N. Konno, “A new time-series model based on quantum walk,” *Quantum Studies: Mathematics and Foundations*, vol. 6, no. 1, pp. 61–72, 2019.
- [22] J. K. Asbóth and H. Obuse, “Bulk-boundary correspondence for chiral symmetric quantum walks,” *Physical review B*, vol. 88, no. 12, p. 121406, 2013.
- [23] H. Obuse, J. K. Asbóth, Y. Nishimura, and N. Kawakami, “Unveiling hidden topological phases of a one-dimensional hadamard quantum walk,” *Physical review B*, vol. 92, no. 4, p. 045424, 2015.
- [24] L. Matsuoka, A. Ichihara, M. Hashimoto, and K. Yokoyama, “Theoretical study for laser isotope separation of heavy-element molecules in a thermal distribution,” in *Proceedings of the International Conference Toward and Over the Fukushima Daiichi Accident (GLOBAL 2011)*, no. 392063, Jul 2011.
- [25] A. Ichihara, L. Matsuoka, E. Segawa, and K. Yokoyama, “Isotope-selective dissociation of diatomic molecules by terahertz optical pulses,” *Physical Review A*, vol. 91, no. 4, p. 043404, 2015.
- [26] J. Wang and K. Manouchehri, “Physical implementation of quantum walks,” *Heidelberg, Springer Berlin*, vol. 10, pp. 978–3, 2013.

- [27] Y. Ide, N. Konno, S. Matsutani, and H. Mitsuhashi, “New theory of diffusive and coherent nature of optical wave via a quantum walk,” *Annals of Physics*, vol. 383, pp. 164–180, 2017.
- [28] T. Yamagami, E. Segawa, and N. Konno, “General condition of quantum teleportation by one-dimensional quantum walks,” *Quantum Information Processing*, vol. 20, no. 7, pp. 1–24, 2021.
- [29] Y. Wang, Y. Shang, and P. Xue, “Generalized teleportation by quantum walks,” *Quantum Information Processing*, vol. 16, no. 9, pp. 1–13, 2017.
- [30] C. Vlachou, W. Krawec, P. Mateus, N. Paunković, and A. Souto, “Quantum key distribution with quantum walks,” *Quantum Information Processing*, vol. 17, pp. 1–37, 2018.
- [31] A. M. Childs, “Universal computation by quantum walk,” *Physical review letters*, vol. 102, no. 18, p. 180501, 2009.
- [32] A. M. Childs, D. Gosset, and Z. Webb, “Universal computation by multiparticle quantum walk,” *Science*, vol. 339, no. 6121, pp. 791–794, 2013.
- [33] H. Robbins, “Some aspects of the sequential design of experiments,” *Bulletin of the American Mathematical Society*, vol. 58, no. 5, pp. 527–535, 1952.
- [34] N. D. Daw, J. P. O’dohererty, P. Dayan, B. Seymour, and R. J. Dolan, “Cortical substrates for exploratory decisions in humans,” *Nature*, vol. 441, no. 7095, pp. 876–879, 2006.
- [35] R. S. Sarkar, A. Mandal, and B. Adhikari, “Periodicity of lively quantum walks on cycles with generalized grover coin,” *Linear Algebra and its Applications*, vol. 604, pp. 399–424, 2020.
- [36] Q. Han, N. Bai, Y. Kou, and H. Wang, “Three-state quantum walks on cycles,” *International Journal of Modern Physics B*, vol. 36, no. 15, p. 2250075, 2022.
- [37] L. Lai, H. El Gamal, H. Jiang, and H. V. Poor, “Cognitive medium access: Exploration, exploitation, and competition,” *IEEE transactions on mobile computing*, vol. 10, no. 2, pp. 239–253, 2010.
- [38] S.-J. Kim, M. Naruse, and M. Aono, “Harnessing the computational power of fluids for optimization of collective decision making,” *Philosophies*, vol. 1, no. 3, pp. 245–260, 2016.
- [39] P. Auer, N. Cesa-Bianchi, Y. Freund, and R. E. Schapire, “Gambling in a rigged casino: The adversarial multi-armed bandit problem,” in *Proceedings of IEEE 36th annual foundations of computer science*, pp. 322–331, IEEE, 1995.